

SCIENCE & TECHNOLOGY

Journal homepage: http://www.pertanika.upm.edu.my/

Optimisation and Predictive Modelling of Natural Frequencies on Carbon/Glass Hybrid Composite Laminates

Abdul Azim Taredi, Siti Mariam Abdul Rahman, Mohd Nor Azmi Ab Patar and Jamaluddin Mahmud*

School of Mechanical Engineering, College of Engineering, Universiti Teknologi MARA, 40450 Shah Alam, Selangor, Malaysia

ABSTRACT

A hybrid laminated composite is a laminate formed by integrating composite layers from various fibre types to achieve optimal properties. Nonetheless, considerable knowledge remains to be acquired regarding the vibration behaviour associated with the hybridisation of composite laminates. In structural design, natural frequency is a critical factor for preventing resonance, which may result in significant structural failure. This study aims to assess the inherent natural frequency response of hybrid composite laminates under free vibration, influenced by varying plate thicknesses, layer fractions, and orientation angles. Finite element models were developed using a commercial finite element software, ANSYS, to precisely characterise the natural frequencies of hybrid composite laminates under free vibration. The design of experiments was employed to identify 17 case study runs and to assess significant factors, with a comprehensive examination of each factor's impact on natural frequencies conducted through modal analysis. Given the limited dataset, employing techniques such as cross-validation with response surface methodology (RSM) and artificial neural networks (ANN) enhances the reliability of performance assessment for the model. Optimisation

ARTICLE INFO

Article history: Received: 23 November 2024

Accepted: 18 May 2025 Published: 08 October 2025

DOI: https://doi.org/10.47836/pjst.33.6.09

E-mail addresses:

2024631962@student.uitm.edu.my (Abdul Azim Taredi) mariam4528@uitm.edu.my (Siti Mariam Abdul Rahman) azmipatar@uitm.edu.my (Mohd Nor Azmi Ab Patar) jm@uitm.edu.my (Jamaluddin Mahmud)

* Corresponding author

was conducted utilising RSM via analysis of variance, while ANN serves as a tool to ascertain data accuracy. The accuracy and robustness of the models are corroborated by a comparison of predictions from finite element analysis and RSM, demonstrating a strong correlation with percentage errors of 16 and 10% for ANN, respectively.

Keywords: ANSYS, artificial neural network, finite element analysis, hybrid composite laminate, natural frequency, response surface methodology

INTRODUCTION

Plate and shell structures are extremely significant and efficient load-bearing entities in various mechanical, aerospace, and civil engineering applications. Being thin-walled structures, they enable the designer to achieve substantial weight savings. The past few decades have witnessed the replacement of traditional materials with multi-layered composite structures such as laminates and sandwich panels, primarily due to their high stiffness-to-weight and flexural rigidity-to-weight ratio, respectively (Sai Vivek, 2016). Vibration analysis of rectangular plates has received considerable attention and has been the subject of numerous studies, which are well documented by Leissa (1973), who classified the accurate results for free vibration frequencies of all 21 combinations of classical boundary conditions for rectangular plates. Free vibration of isotropic and orthotropic rectangular plates with mixed boundary conditions is investigated by Mirziyod et al. (2019). Conducting physical experiments can be expensive, particularly when working with largescale systems or processes. Simulation allows for the modelling of these systems without the need for physical experiments, which can significantly reduce the cost effectively. This is relevant to Industry 4.0, where a global survey with more than 2,000 respondents suggests that approximately 5% of a company's annual revenue will be invested in digitalisation projects (de Paula Ferreira et al., 2020). Over the past few decades, finite element modelling (FEM) has been used more often to support engineering projects because of its inexpensive prices, reduced project elaboration time, and improved computational and data-processing capabilities (Müzel et al., 2020). Solid elements are the least employed in composites since they necessitate a multi-layered model or an expensive, time-consuming full-size construction, which makes them impractical (Chisena et al., 2021).

In recent years, the integration of composite materials has gained significant attention across various industries, particularly due to their superior structural performance and vibration characteristics. Hybrid composites, which are combinations of various fibre materials, have exhibited significant potential in aerospace, automotive, construction and consumer sectors. The natural frequency refers to the dynamic properties, exhibiting the level of vibration in relation to the mass and stiffness of a structure (Alam et al., 2020; Norman & Mahmud, 2021). Comprehending natural frequencies and mode shapes is essential for averting sudden and catastrophic failures, as each structure possesses distinct resonant frequencies (An et al., 2019; Ratnaparkhi & Sarnobat, 2013). This paper considers the frequencies of hybrid composites of rectangular full plates subjected to free vibration. During vibration, spots on the plate undergo small displacements in the direction perpendicular to the plane of the plate (Warburton, 1954).

Composite plates play a vital role, particularly in hybrid laminates, where the stacking sequence, fibre orientation, and material selection profoundly influence dynamic response (B. S. Reddy et al., 2013; Jadee et al., 2020). Recent studies have delved into various

factors influencing the vibration behaviour of hybrid composites. For instance, Li et al. (2024) performed an extensive analysis of carbon/glass hybrid composites laminated plates under various boundary conditions, emphasising the influence of hybrid ratio, stacking sequences, and fibre orientations on their vibrational properties. Ma and Gao (2024) investigated the free vibration of hybrid laminated thin-walled cylindrical shells composed of multilayer functionally graded carbon nanotube-reinforced composite plies, highlighting the significance of material gradation in dynamic performance. A study by Sreekanth et al. (2023) discussed the initiation of delamination that had caused the major failure of laminated composite structures, affected by the dynamic characteristics and vibration properties. Likewise, Bulut et al. (2016) and Quanjin et al. (2022) conducted physical tests and numerical simulations for free vibrations of Kevlar/glass epoxy laminated composite plates. Arvinda Pandian and Jailani (2021) investigated the mechanical and thermal properties of hybrid epoxy laminates reinforced with jute and linen fabrics along with fumed silica filler, highlighting how material composition influences composite behaviour. Erklil et al. (2015) also examined the influence of hybridisation on natural frequency through experiment and simulation. Norman et al. (2018) investigated the free vibrations of the laminated composite beam, analysing the influence of different lamination schemes using ANSYS software. Shi et al. (2020) developed an analytical approach for examining free vibrations of cross-ply Glass/epoxy composite laminates with shallow shells by incorporating a semi-analytic method into arbitrary classical and elastic boundary conditions. There are also studies related to free vibrations of hybrid laminated composite plates. A study showed that the matrix material, hybridisation, and laminate stacking sequence affect the natural frequencies and mode shapes. These studies cover diverse areas, including the exploration of the impact of varying fibre volume fraction ratios, as demonstrated by Pushparaj and Suresha (2016). Finite element analysis (FEA) was used by Crawley (1979) in the numerical approach, and the outcomes of the experiments were compared. However, there is still much to learn about natural frequencies in hybrid composites, even though previous studies have illuminated a number of these topics (Safri et al., 2018).

Therefore, this paper aims to investigate the influence factors of natural frequency response to hybrid composite, and the optimum factors are also determined by implementing the RSM. Optimising process factors is a significant challenge in experimental work, crucial for conserving resources, reducing costs, and achieving improved outcomes. To do so, the advanced statistical tools must be adopted within the investigation. RSM is a sophisticated design of experiments (DOE) technique that involves statistical modelling to develop and analyse processes, with the goal of optimising the desired response influenced by multiple input factors (Alam et al., 2020; Bezerra et al., 2008; Shokuhfar et al., 2008; Swamy et al., 2014). Using the DOE approach reduced the number of necessary experiments while still

enabling the collection of significant amounts of data. When compared to the sequential variation of one factor at a time, this approach enabled the concurrent exploration of multiple factors, resulting in a significant reduction in the time and resources required (Antony, 2014). Implement the Box-Behnken design (BBD) technique; the experimental layout was created with three factors, each with three levels. The BBD was proposed by George E. P. Box and Donald W. Behnken in 1960. Their objective was to develop an effective experimental design methodology capable of accommodating second-order (quadratic) models without necessitating the extensive number of experiments required for a complete three-level factorial design (Box & Behnken, 1960). Thus, the design is a great option for maximising the natural frequency of hybrid composite laminates because it works particularly well for building second-order polynomial models and investigating quadratic response surfaces (Triefenbach, 2008). Thus, BBD provides the most information with their greater symmetry and rotatability and requires fewer experimental runs (Antony, 2014). This design offers a thorough understanding of the interactions between variables by simultaneously varying multiple factors, which produces more robust and trustworthy results. Nonetheless, although RSM provides interpretable models, its prediction accuracy may be constrained when addressing highly nonlinear and intricate connections frequently encountered in hybrid composite structures (Saravanakumar et al., 2024).

The last few decades have focused a lot of emphasis on the integration of composite materials in a variety of applications, especially regarding their structural performance and vibration characteristics. According to a recent study, the use of ANN modelling is becoming more common and may even reduce process complexity (Subrahmanyam et al., 2021). For instance, studies have investigated using ANN as a failure structure prediction tool (Kumar C & Swamy, 2021; Norman et al., 2022; Sreekanth et al., 2023). Neural networks are constructed by connecting neurons through weighted interconnections, and the most critical step is determining these weights, a process known as training. In developing the ANN model, the Levenberg-Marquardt (LM) algorithm has gained popularity among studies, as it has proven efficiency in training feed-forward networks for vibration analysis of composite structures. Previous studies have demonstrated the algorithm's effectiveness in predicting vibration response under varying environmental conditions with high accuracy (Kallannavar et al., 2020). Other studies developed an ANN model using a multilayer perceptron (MLP) with backpropagation to predict the natural frequencies of laminated composite plates with higher accuracy (M. R. S. Reddy et al., 2012). However, smaller datasets may pose a risk of overfitting if not managed properly. In this context, Arunachalam et al. (2024) conducted experiments and simulation analysis on predicting the hardness and strength of the polymer composite by applying silane treatment. Optimisation of RSM was done by indicating the influence factor and ANN to predict the flexural strength and hardness. Even though the small dataset produced a high of 95% accuracy of predictions by using an ANN. Mallick et al. (2024) investigate an electroless nickel-phosphorus (Ni–P) coating's ability to withstand corrosion on a copper substrate using BBD and ANN. It has 17 data sets given by BBD, where 70% of the data have been used for input, 15% for testing and 15% for validation. BBD produces 87% accuracy, and 88% for ANN.

In this study, the plate thickness, layer fraction, and lamination schemes have been considered as the three factors to be optimised using BBD to achieve optimal natural frequencies of a hybrid composite laminate. The natural frequencies provide insight into the vibrational behaviour and structural integrity of the carbon/glass under various conditions. Additionally, a predictive model can be useful to predict the natural frequencies of this hybrid composite across multiple values of input factors. To identify the significant factors in this process, analysis of variance (ANOVA), a robust statistical tool, has been employed to analyse residuals, detect outliers, and evaluate the validity of the developed model. Furthermore, a more precise predictive model for identifying the best-fit natural frequency responses of the hybrid composite laminates has been established using an ANN.

METHODOLOGY

Mesh Convergence Analysis and Numerical Validation

Mesh Convergence Analysis

In finite element analysis, mesh convergence analysis is essential for determining the optimal mesh size to achieve a balance between accuracy and computational efficiency (Samsudin & Mahmud, 2015). To verify that the simulation results converge to a stable solution, it assesses the sensitivity of numerical outcomes to variations in mesh size. As a result, a range of mesh sizes was employed. 1×2 , 2×4 , 3×6 , 4×8 , 5×10 , 6×12 , 7×14 , 8×16 , and 16×32 . The mesh employs a quadrilateral configuration on a model measuring 150 mm in length and 75 mm in width, utilising the shell element type 8 node 281. This stage encompassed a range of angles from 0° to 90° and employed symmetric angle lamination $[\theta^{\circ}/-\theta^{\circ}/\theta^{\circ}/-\theta^{\circ}]$ s as the stacking configuration. This aims to ascertain the behaviour of natural frequencies and the deformed shape.

Numerical Validation

The purpose of numerical validation is to confirm the accuracy of free vibration analysis for a hybrid laminated composite by validating the finite element model using ANSYS *Parametric Design Language* (APDL) (v16.0, SAS IP, Inc., USA). The validation procedure is founded on the work of (Pushparaj & Suresha, 2016) and the study conducted by Norman and Mahmud (2021). The hybrid composite consists of E-glass/T300 carbon epoxy plates (Pushparaj & Suresha, 2016) measuring 150 mm in length and 75 mm in width. Figure 1 illustrates the dimensions and clamped-free-free (CFFF) boundary condition of the

plate. The ply thickness of the T300 carbon fibre lamina is 0.13 mm, whereas the E-glass fibre lamina has a ply thickness of 0.15 mm. The plate consists of 8 layers, which were divided into 400 elements using eight-node quadrilateral shell elements, namely SHELL 281, and the material properties are tabulated in Table 1. The lamination angle is [0g/+45c/45c/90g]s and [0c/+45g/-45g/90c]s was examined. Thus, the first five mode shapes and natural frequencies of the plate are used in the Block Lanczos mode extraction method.

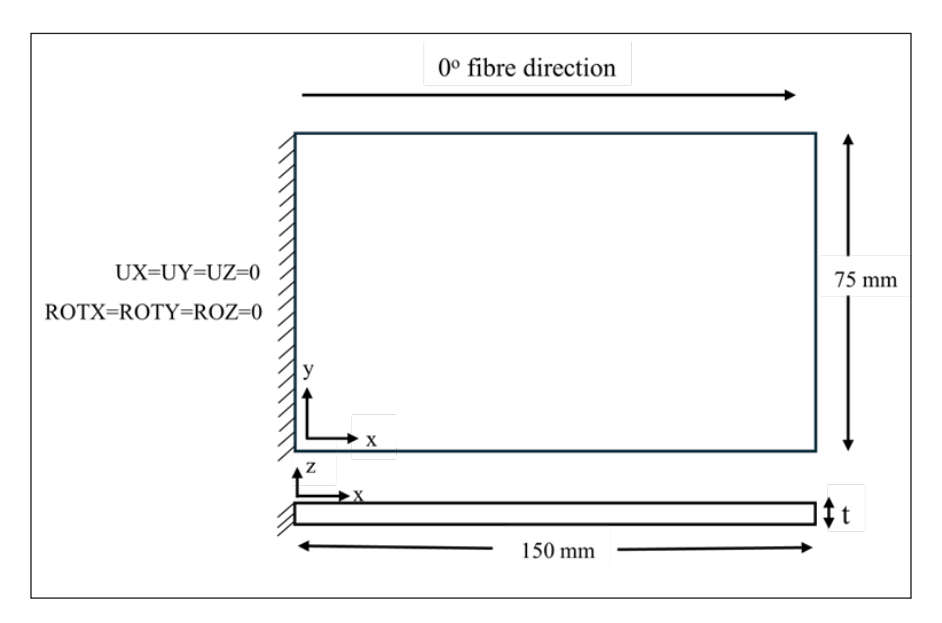


Figure 1. Rectangular plate configuration

Note. UX = Displacement in x-direction; UY = Displacement in y-direction; UZ = Displacement in z-direction; ROTX = Rotation about x-axis; ROTY = Rotation about y-axis; ROTZ = Rotation about z-axis; t = Thickness of the laminate, which is varied depending on the number of laminas

Table 1
Material properties of T-300 carbon epoxy (Samsudin & Mahmud, 2015) and E-glass epoxy (Pushparaj & Suresha, 2016)

| T-300 carbon epoxy | Values | E-glass epoxy | Values | |
|--------------------|------------------------|-------------------|------------------------|--|
| E_1 | 132.4 GPa | E_{1} | 44.93 GPa | |
| $E_2 = E_3$ | 10.76 GPa | $E_2 = E_3$ | 14.04 Gpa | |
| $V_{12} = V_{13}$ | 0.24 | $V_{12} = V_{13}$ | 0.2481 | |
| V_{23} | 0.49 | V_{23} | 0.3775 | |
| $G_{12} = G_{13}$ | 5.645 GPa | $G_{12} = G_{13}$ | 5.263 Gpa | |
| G_{23} | 3.38 GPa | G_{23} | 5.101 Gpa | |
| ρ | $1,600 \text{ kg/m}^3$ | ρ | $2,081 \text{ kg/m}^3$ | |

Note. E_1 = Longitudinal Young's modulus; E_2 = Transverse Young's modulus; E_3 = Through-thickness Young's modulus; E_3 = Poison ratio in 1-2 plane, E_3 = Poison ratio in 1-3 plane; E_3 = Poison ratio in 2-3 plane; E_3 = Shear modulus in 1-2 plane; E_3 = Shear modulus in 1-3 plane; E_3 = Shear modulus in 2-3 plane; E_3 = Density

Set Up Factors Using the DOE and Vibration Analysis

Statistical optimisation was conducted using the BBD implemented in Design Expert (22.0.6 64-bit) to optimise factors for symmetric configurations as shown in Table 2. At least three continuous elements are needed for this cubic design, which is defined by the midpoints of the edges of a multi-dimensional cube. In this study, the effects of three numerical factors, namely fibre angle orientation (θ°), layer fraction (Lf, %) and plate thickness (t, mm), on the natural frequencies of the hybrid composite laminate were investigated. The laminate consists of 8 layers arranged in a symmetric lamination scheme of $[\theta^{\circ}/-\theta^{\circ}/\theta^{\circ}/-\theta^{\circ}]$ s. For variation, the minimum and maximum levels were set as follows: $\theta = 0^{\circ}$ to 45° , Lf = 0 (0%) to 1 (100%) and t = 0.5 to 3 mm, corresponding to fibre angle orientation, layer fraction and plate thickness, respectively. The layer fraction represents the percentage of carbon/epoxy lamina: a value of '0' indicates that all eight layers are made of glass/epoxy, '0.5' indicates that there are four layers of carbon/epoxy and four layers of glass/epoxy, and '1' indicates all eight layers are carbon/epoxy. In all cases, the stacking sequence follows the $[\theta^{\circ}/-\theta^{\circ}/\theta^{\circ}/-\theta^{\circ}]$ s configuration.

The finite element model is constructed as illustrated in Figure 1 using APDL (v16.0, SAS IP, Inc., USA) for the numerical validation. The properties of the materials, as well as additional DOE-set factors, are applied. The shell 281 elements are the same as in the first stage, and CFFF for boundary conditions are used.

Table 2
Box Behnken configuration

| Variables | Low (-) | Middle (0) | High (+) |
|---------------------------|---------|------------|----------|
| A: Angle orientation (θ°) | 0 | 22.50 | 45 |
| B: Layer fraction (%) | 0 | 0.50 | 1 |
| C: Plate thickness (mm) | 0.50 | 1.75 | 3 |

Optimisation Using RSM

In this phase, the link between controllable input elements and the generated response surfaces is characterised using RSM. The methodical examination of the impacts of several variables and their interactions, RSM, which is backed by Design Expert software (22.0.6 64-bit), allows for a thorough study of input-output data and makes it easier to optimise the response variable. ANOVA is used in the BBD model to evaluate each component's statistical significance and how it interacts with the response. ANOVA is crucial for determining which factors have a significant influence on the response and for confirming the model's robustness. Regression equations and contour plots are created to show and analyse the relationships between input and output variables based on findings from previous stages.

Prediction of Natural Frequency Using ANN

The first step in using an ANN to predict natural frequencies was gathering and preprocessing response data from simulation samples. The natural frequencies of DOE samples were examined by using ANSYS. This ensures the neural network model can operate with the data, which encompasses a variety of factors and their corresponding responses and has been normalised by Malik and Arif (2013). This study's ANN model was trained via the LM algorithm, a powerful optimisation method recognised for its swift convergence and low mean squared error (MSE) in small to medium datasets (Kallannavar et al., 2020). The dataset produced by the BBD was randomly partitioned into 70% for training, 15% for validation, and testing to ensure model generalisation and mitigate overfitting (Boukarma et al., 2023; Subrahmanyam et al., 2021). The model's prediction accuracy was evaluated using Equation 1, MSE and Equation 2, root mean squared error (RMSE) metrics, where MSE measures the average of the squares of the differences between the predicted \hat{y}_i and actual y_i values. Thus, RMSE provides an error value in the same units as the original outputs, measuring how accurately the prediction model performs. The input values were the predetermined variables for BBD, which are as follows: angle orientation (A), layer fraction (B), and plate thickness (C), as shown in Figure 2.

$$MSE = \frac{1}{n} \sum_{i=1}^{n} (\hat{y}_i - y_i)^2$$
 [1]

$$RMSE = \sqrt{\frac{1}{n} \sum_{i=1}^{n} (\hat{y}_i - y_i)^2}$$
 [2]

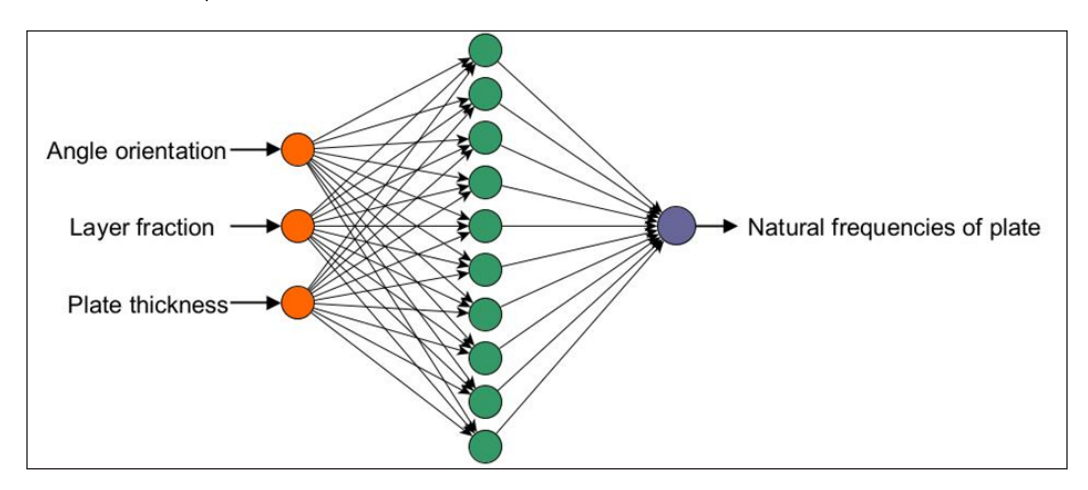


Figure 2. Architecture of the proposed artificial neural network predictive model

RESULTS AND DISCUSSION

Mesh Convergence and Numerical Validation

Convergence Analysis

The results obtained from the mesh convergence analysis are shown in Figure 3. The different mesh sizes in hybrid laminated composites are responsible for the slight differences in natural frequencies. The results plateau at mesh sizes larger than 8x16, or 128 elements, suggesting that the effect on natural frequencies is negligible. Therefore, for the ensuing analyses, an 8×16 mesh was used for this study. Interestingly, it is worth noting that these findings are particular to dataset mode number 5.

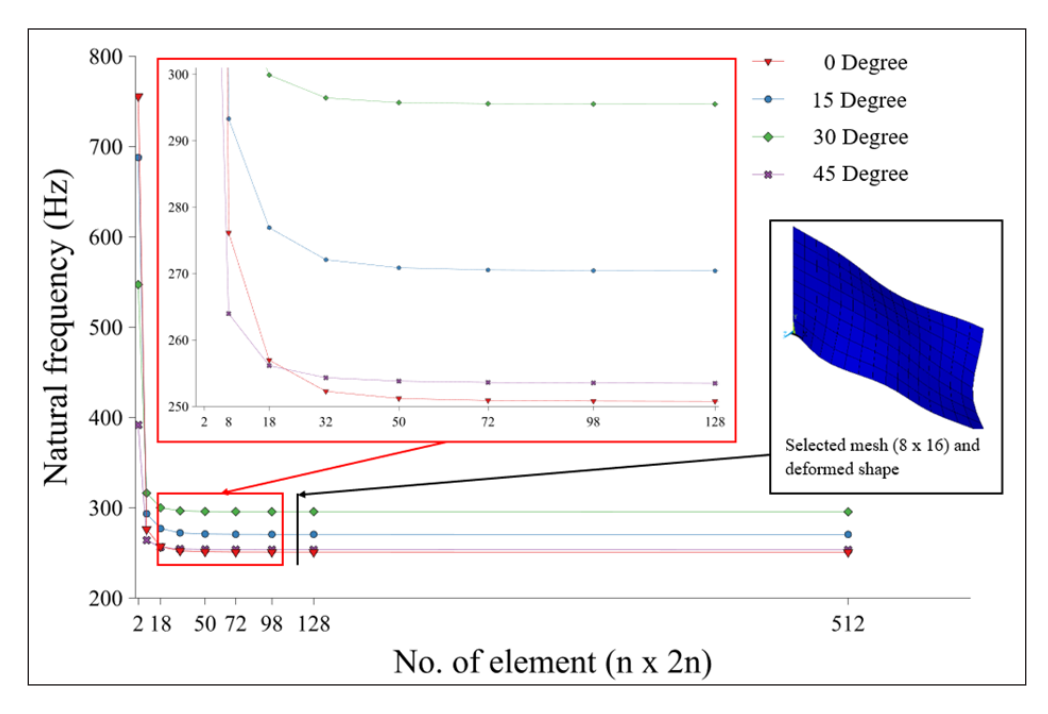


Figure 3. Convergence analysis of the mesh for the hybrid composite plate [0g/+45c/-45c/90g]s

Numerical Validation

Table 3 compares the results of this simulation to (Pushparaj & Suresha, 2016). The acquired natural frequencies and the mode shapes of the hybrid T300 carbon/E-glass epoxy were compared. The data indicates a modulus value with the maximum true error recorded at under 5.02%. The findings indicate that changes in lamina sequences result in differences in mode shapes, although they resemble those identified in the previous study. The literature indicates that this study demonstrated a significant level of agreement in the similarity response.

Table 3
Comparison of simulated natural frequencies and mode shapes with literature

| Lamination scheme | Mode | Pushparaj and Suresha (2016) | Present study | True error (%) |
|--------------------|------------|---------------------------------|---------------------------|-------------------|
| | | Numerical simulation (Hz) | Numerical simulation (Hz) | _ |
| [0g/45c/-45c/90g]s | 1 Bending | 37.374 | 37.465 | 0.24 |
| | 1 Torsion | 165.05 | 162.74 | 1.40 |
| | 2 Bending | 231.26 | 232.18 | 0.40 |
| | 2 Torsion | 550.26 | 522.61 | 5.02 |
| | 1 Combined | 645.65 | 648.03 | 0.37 |
| [0c/45g/-45g/90c]s | 1 Bending | 54.697 | 53.277 | 2.60 |
| | 1 Torsion | 137.08 | 139.62 | 1.85 |
| | 2 Bending | 341.24 | 332.42 | 2.58 |
| | 2 Torsion | 495.24 | 497.9 | 0.54 |
| | 1 Combined | 654.26 | 670.86 | 2.54 |

DOE Factors and Vibration Analysis

This result was generated using the BBD, which was employed to classify the three factors of the experiment. It set the case study that involved developing 17 simulations, all of which had to be completed using FEA. This result contains angle orientation $[\theta^{\circ}/-\theta^{\circ}/\theta^{\circ}]$ s for symmetric with fixed variable layer fraction 0,0.5, and 1, then thickness from 0.5 to 3 mm, and angle of orientation 0° until 45°. For a hybrid arrangement, the layup is [C, G, C, G, C, G, C], where C is carbon and G is glass. Table 4 shows the completed value of FEA for the symmetric.

Table 4
Natural frequencies for symmetric laminate

| Run | Factor 1 A: Angle of orientation (Degree) | Factor 2 B: Layer fraction (%) | Factor 3 C: Plate thickness (mm) | FEA | RSM | ANN | Error of RSM (%) | Error of ANN (%) |
|-----|--|---|---|--------|--------|-------|---------------------|---------------------|
| 1 | 0 | 0.5 | 0.50 | 27.18 | 24.31 | 30.11 | 10.56 | 10.78 |
| 2 | 0 | 0.5 | 3.00 | 162.77 | 161.75 | 162.9 | 0.63 | 0.08 |
| 3 | 22.5 | 0 | 3.00 | 88.06 | 86.59 | 88.89 | 1.67 | 0.94 |
| 4 | 45 | 0 | 1.75 | 38.00 | 38.00 | 37.97 | 0.00 | 0.09 |
| 5 | 0 | 1 | 1.75 | 114.38 | 122.38 | 114.4 | 7.00 | 0.02 |
| 6 | 45 | 0.5 | 0.50 | 12.95 | 15.07 | 13.94 | 16.33 | 7.63 |
| 7 | 22.5 | 0.5 | 1.75 | 72.50 | 70.50 | 72.70 | 2.75 | 0.14 |
| 8 | 22.5 | 0.5 | 1.75 | 72.50 | 70.50 | 72.70 | 2.75 | 0.14 |
| 9 | 22.5 | 0.5 | 1.75 | 72.50 | 70.50 | 72.70 | 2.75 | 0.14 |
| 10 | 22.5 | 0.5 | 1.75 | 72.50 | 70.50 | 72.70 | 2.75 | 0.14 |
| 11 | 22.5 | 0 | 0.50 | 14.71 | 15.09 | 15.00 | 2.55 | 1.95 |

Table 4 (continue)

| Run | Factor 1 A: Angle of orientation (Degree) | Factor 2 B: Layer fraction (%) | Factor 3 C: Plate thickness (mm) | FEA | RSM | ANN | Error of RSM (%) | Error of ANN (%) |
|-----|--|---|---|--------|--------|--------|---------------------|---------------------|
| 12 | 22.5 | 1 | 3.00 | 160.54 | 156.05 | 161.00 | 2.80 | 0.29 |
| 13 | 45 | 0.5 | 3.00 | 76.93 | 80.89 | 83.16 | 5.15 | 8.10 |
| 14 | 45 | 1 | 1.75 | 54.94 | 57.96 | 55.08 | 5.49 | 0.26 |
| 15 | 0 | 0 | 1.75 | 58.69 | 63.67 | 54.95 | 8.50 | 6.37 |
| 16 | 22.5 | 1 | 0.50 | 26.93 | 24.29 | 29.77 | 9.81 | 10.53 |
| 17 | 22.5 | 0.5 | 1.75 | 72.50 | 70.50 | 72.60 | 2.75 | 0.14 |

Note. FEA = Finite element analysis; RSM = Response surface methodology; ANN = Artificial neural network

The modal analysis employing the Block Lanczos method yielded multiple mode shapes and natural frequencies, derived from a specified number of modes for extraction. Each mode shape displayed distinct deformation types, such as torsion, bending, or a combination of both. The selection of the first natural frequency is based on the mode shape of the first bending mode, as shown in Figure 4 (a). The second natural frequency aligns with the

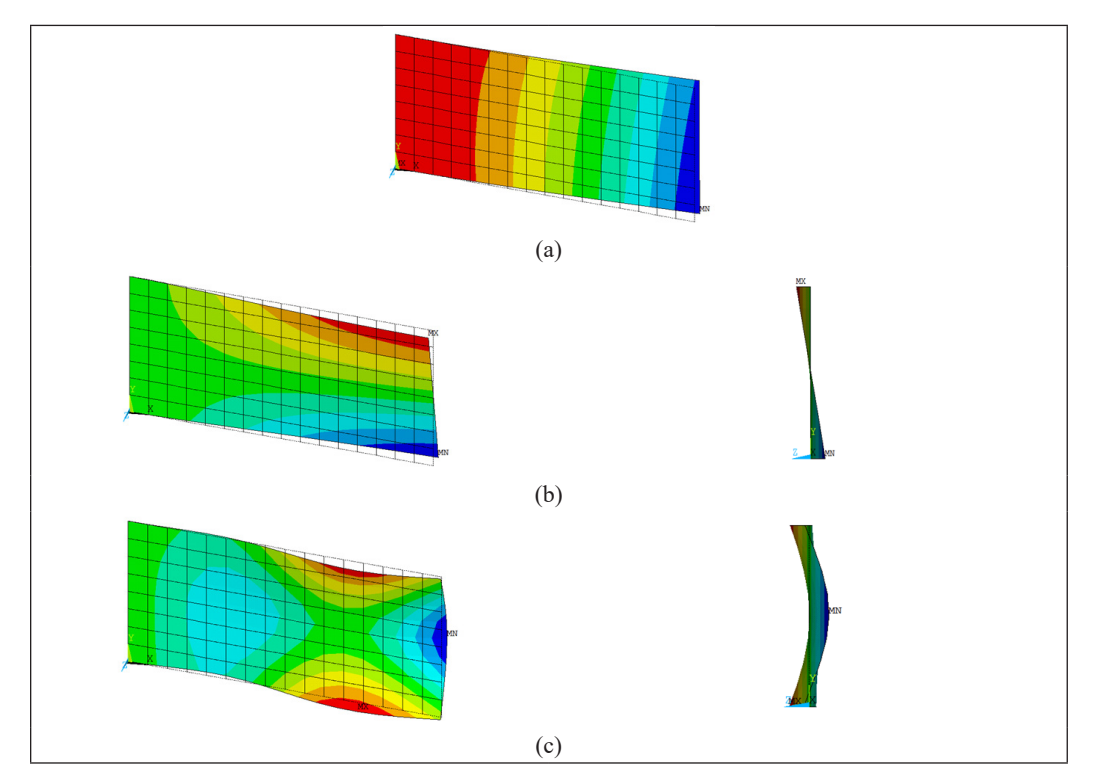


Figure 4. Classification of mode: (a) 1 bending, (b) 1 torsion, and (c) 1 combined *Note*. X = x-axis; Y = y-axis; Z = z-axis; MN = Minimum; MX = Maximum

initial torsion mode depicted in Figure 4 (b), and the third natural frequency represents the combined torsion and bending mode, illustrated in Figure 4 (c). This deformation is verified by Pushparaj and Suresha (2016) and is comparable to the work of Merzuki et al. (2019), Njim et al. (2021), Norman et al. (2018), and Norman and Mahmud (2021). The mode shapes were deformed in exact alignment in accordance with both the experimental and numerical findings, demonstrating a remarkable level of concordance in this study.

Optimisation Using RSM

ANOVA based on the BBD was performed with Design Expert software to check the adequacy and significance of the model coefficients (Mallick et al., 2024; Mengistu et al., 2024; Rosaidi et al., 2023). An actual Equation3 was formulated through the ANOVA after the evaluation of the FEA model. This equation yielded the prediction of natural frequencies. Thus, Equation 3 is for a symmetric case (f₁) where A is the angle of orientation, B is the layer fraction, and C is the plate thickness. Table 5 shows the efficacy of the RSM model in predicting natural frequencies, with most of the percentage error comparatively minimal. The maximum error in the symmetric laminate does not surpass 17%, indicating a high level of accuracy at samples with an average percentage error of 4.96%. The RSM model performs well at two-factor interaction (2FI), especially regarding smaller percentage errors, thereby validating its use in vibration analysis of composite structures. High coefficients of determination, $R^2 = 1$, indicate a good correlation between the measured and predicted response when it is closely aligned (Boukarma et al., 2023; Polat & Sayan, 2019). If the p-value of any process factor or its interactions is below 0.05, it can be concluded that those factors or their interactions are significant (Mallick et al., 2024; Mengistu et al., 2024; Rosaidi et al., 2023).

$$f_1(symmetric) = -11.44205 + 0.543536A + 16.52975B + 42922.49C$$
$$-0.861311AB - 636.54133AC + 24104BC$$
[3]

where f_1 = a symmetric case, A = angle of orientation, B = layer fraction, and C = plate thickness.

A substantial F-value and minimal p-value indicate that each term exerts a significant influence (Mat Jusoh et al., 2024; Polat & Sayan, 2019). The model's p-value of under 0.0001 and F-value of 286.35 for the symmetric laminate in Table 5 indicate a substantial level of statistical significance. Thus, the lack of fit values was found to be insignificant. The high R^2 value of 0.9942, signifying that 99.42% of the variability in the natural frequencies is

Table 5
Result of the two-factor interaction model for a symmetric laminate

| Source | Sum of | Df | Mean | F-value | <i>p</i> -value | |
|-----------------------|----------|----|----------|---------|-----------------|-------------|
| | squares | | square | | | |
| Model | 30375.74 | 6 | 5062.62 | 286.35 | < 0.0001 | Significant |
| A - Angle orientation | 4058.65 | 1 | 4058.65 | 229.56 | < 0.0001 | |
| B - Layer fraction | 3094.05 | 1 | 3094.05 | 175.00 | < 0.0001 | |
| C - Plate thickness | 20657.63 | 1 | 20657.63 | 1168.43 | < 0.0001 | |
| AB | 375.57 | 1 | 375.57 | 0.00 | 0.0010 | |
| AC | 1282.03 | 1 | 1282.03 | 21.24 | < 0.0001 | |
| BC | 907.82 | 1 | 907.82 | 72.51 | < 0.0001 | |
| Residual | 176.80 | 10 | 17.68 | 51.35 | < 0.0001 | |
| Lack of fit | 176.80 | 6 | 29.47 | | | |
| Pure error | 0.00 | 4 | 0.0000 | | | |
| Cor total | 30552.54 | 16 | | | | |

Note. $R^2 = 0.9942$, $R^2(Adj) = 0.9907$, $R^2(Pred) = 0.9729$, Adeq precision = 54.3630

accounted for by the model, enhances its credibility. The model's robustness and predictive capability are validated by the adjusted R^2 (0.9907) and predicted R^2 (0.9729) values. The adequate precision of 54.3630 signifies a high signal-to-noise ratio, which is beneficial for model accuracy. With an exceptionally high F-value of 1168.43, plate thickness (C) stands out as the most influential factor, indicating its predominant impact on natural frequencies. The angle orientation (A) and layer fraction (B) are highly significant, with F-values of 229.56 and 175.00, respectively, and they substantially contribute to the variation in natural frequencies. The interaction terms (AB, AC, and BC) are significantly notable; the interaction (F-value = 72.51) between plate thickness and layer fraction (AC) highlights the combined effect of these two factors on the natural frequencies.

Figure 5 displays the diagnostic plots typically used to examine the performance of the quadratic model, and to evaluate the ANOVA model (Boukarma et al., 2023). The errors are concentrated along the straight line near the central position, which is predominantly normally distributed. Nevertheless, several residuals exceed the red control limits in Figures 5(b) and 5(d). These points signify regions where the model exhibits overfitting, but the overall randomness of the scatter indicates that the model's assumptions are not severely violated, and keeping the predictions for natural frequencies is generally reliable (Sathishkumar et al., 2022). Figure 5(c) presents a comparison between the actual response values and their corresponding predicted response values generated by the model. The graph of predicted values compared to actual values is significant as it allows the identification of a value or a set of values that the model does not predict accurately.

Figure 6 illustrates the impact of interactions on the response. To accurately identify this effect, the response surface was plotted as a function of two variables, while maintaining the others at their central values. Figures 6(a)-(c) clearly demonstrate that the natural

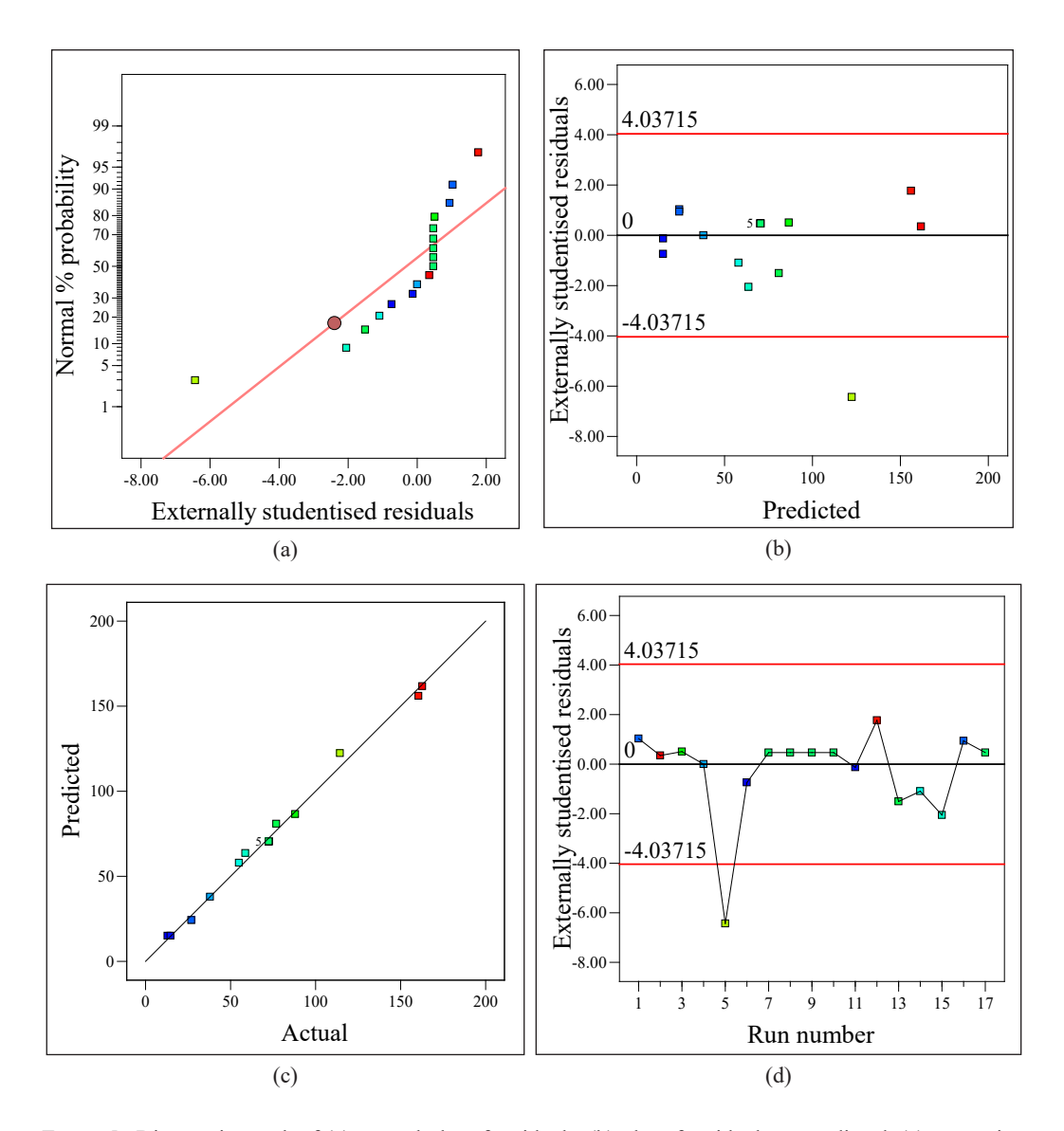


Figure 5. Diagnostic graph of (a) normal plot of residuals, (b) plot of residuals vs predicted, (c) regression analysis of predicted vs actual, and (d) residuals vs run number distribution

frequencies increase with the thickness of the plate. The interactions among the factors can be analysed from the figure, which illustrates that the second-order three-dimensional (3D) response surface plot, along with the contour plot of natural frequencies, corresponds to layer fraction with a lower angle orientation. Figure 6(c) provides a significant influence of the interaction between both factors on the natural frequencies, with colours transitioning from blue, indicating the low-response zone, to red, signifying optimal response. These results align with the findings of (Mat Jusoh et al., 2024). (Boukarma et al., 2023) proposed

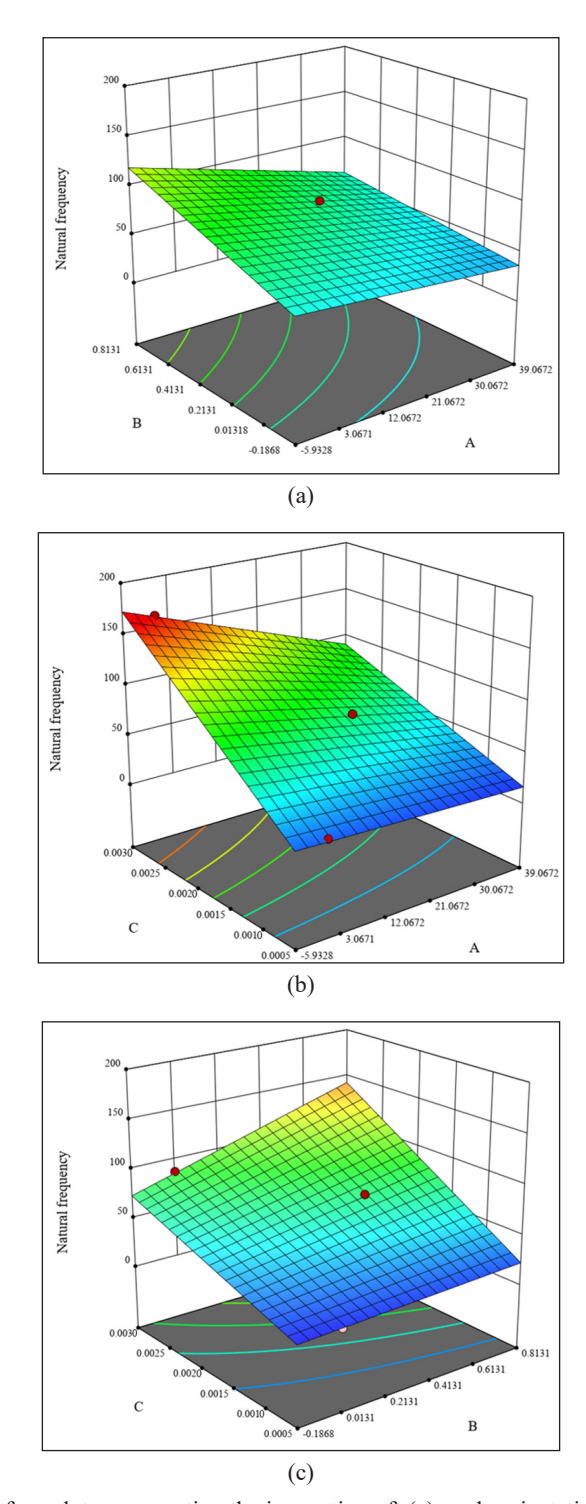


Figure 6. Response surface plots representing the interaction of: (a) angle orientation (A) and layer fraction (B); (b) angle orientation (A) and plate thickness (C); and (c) layer fraction (B) and plate thickness (C)

the solution to ascertain which factors are more significant than others by selecting two points at the minimum and maximum levels on the graph. The first scenario features a minimum plate thickness and a maximum layer fraction (C = 0.0005m, B = 1%), while the second scenario is the inverse (C = 0.003m, B = 0%). The model predicts responses of 26.9 and 88.1 Hz for the two points, respectively.

Prediction of Natural Frequency Using ANN

The regression values are significant as they indicate the model's adequacy in fitting the data. A regression value approaching 1 signifies that the model exhibits high accuracy in predicting natural frequencies. The efficacy of ANN models for predicting natural frequencies in symmetric systems was summarised in Table 6. The ANN model attained a high R^2 (>0.99) and low RMSE (~2.8%), demonstrating superior prediction performance relative to traditional regression techniques. The efficacy of LM and data partitioning techniques has been continuously corroborated in the modelling of composite materials and the prediction of structural dynamics to prevent overfitting (Pratap et al., 2024). The hybrid composite laminate model exhibits a low training MSE of 0, a validation MSE of 35.3960, and a test MSE of 25.6818, indicating exceptional accuracy, supported by high R values of 1.0000 for training, 0.9971 for validation, and 0.9986 for testing.

Table 6
Model summary of an artificial neural network

| Туре | Mean squared error (MSE) | Regression (R) | | |
|------------|-----------------------------|----------------|--|--|
| Training | 0.0000 | 1.0000 | | |
| Validation | 35.3960 | 0.9971 | | |
| Test | 25.6818 | 0.9986 | | |

Figure 7 illustrates the performance graphs of the ANN. The MSE evaluates the performance of the ANN over multiple epochs for training, validation, and test datasets. The optimal validation performance occurred at epoch 3, yielding a MSE of 35.3960. Effective learning is demonstrated by a steady decrease in training error, indicated by the blue line, as the number of epochs increases. This trend aligns with the findings of (Kumar C & Swamy, 2021), who predict the fatigue life of glass fibre, and the study by Mallick et al. (2024) though with a slightly different trajectory in this finding. Result shows the best validation performance for a total of five epochs with stagnant training and gradual increase in both validation and test MSE, like Arunachalam et al. (2024). The validation error on the green line, indicative of the model's generalisation to novel data, initially decreases before reaching a plateau. The test error on the red line, which evaluates the model's generalisation capability, exhibits a similar pattern.

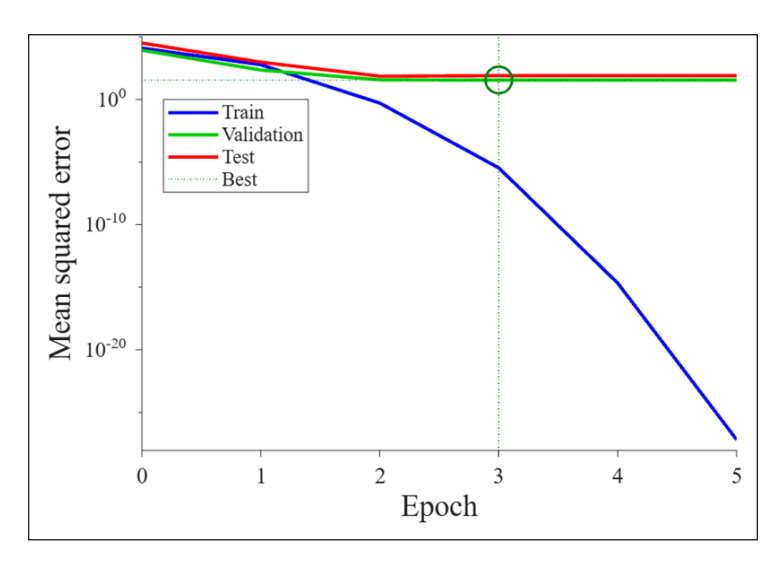


Figure 7. Performance plot of the artificial neural network *Note*. The green circle highlights the best performance that happened at Epoch =3

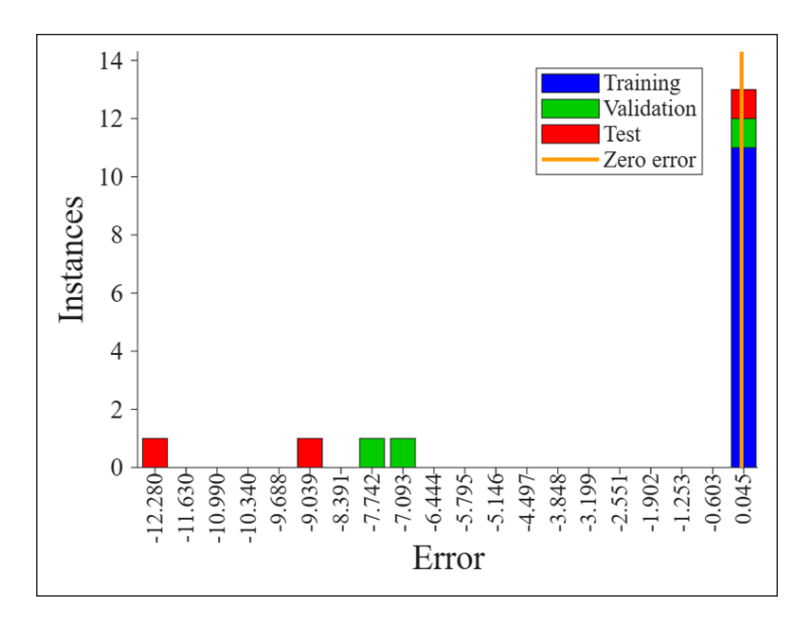


Figure 8. The value of the error histogram Note. The vertical line in orange colour highlights the intersection with the x-axis at error = 0

The error histogram serves as a crucial diagnostic instrument for assessing the reliability and performance of predictive models. The distribution of errors across multiple datasets provides insights into the model's accuracy, generalisability, and potential areas for enhancement. Figure 8 presents error histograms with 20 bins corresponding to the training, validation, and testing phases of the network. The analysis indicates that the

network's predictions exhibit high precision and accuracy, with errors ranging from 0.03 to -0.5 within a narrow interval. Notable errors occur within the negative range, particularly between -12 and -6. The substantial negative errors suggest that, in some instances, the model significantly underestimates the target values. The distribution of test and validation errors across the bins indicates potential effective generalisation of the model; however, further analysis is required to assess overfitting.

Figure 9 presents regression analysis plots for the ANN models employed in predicting natural frequencies. The training dataset exhibits a correlation coefficient of 1, indicating robust model performance throughout the training phase. The test dataset attains an *R* value

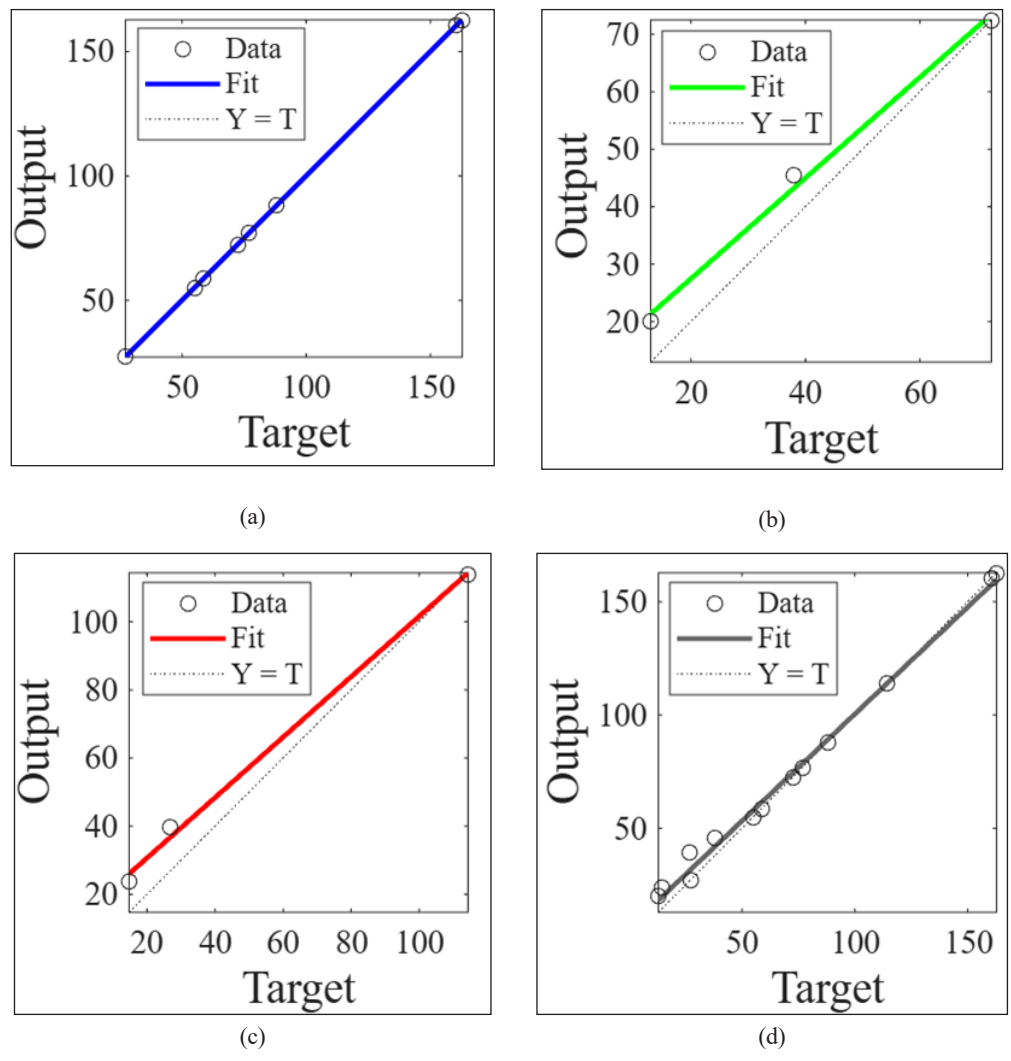


Figure 9. The results for regression analysis: (a) training, (b) validation, (c) test, and (d) overall data *Note*. The dotted line represents the ideal line where the output (Y) = target for a perfect fit (T)

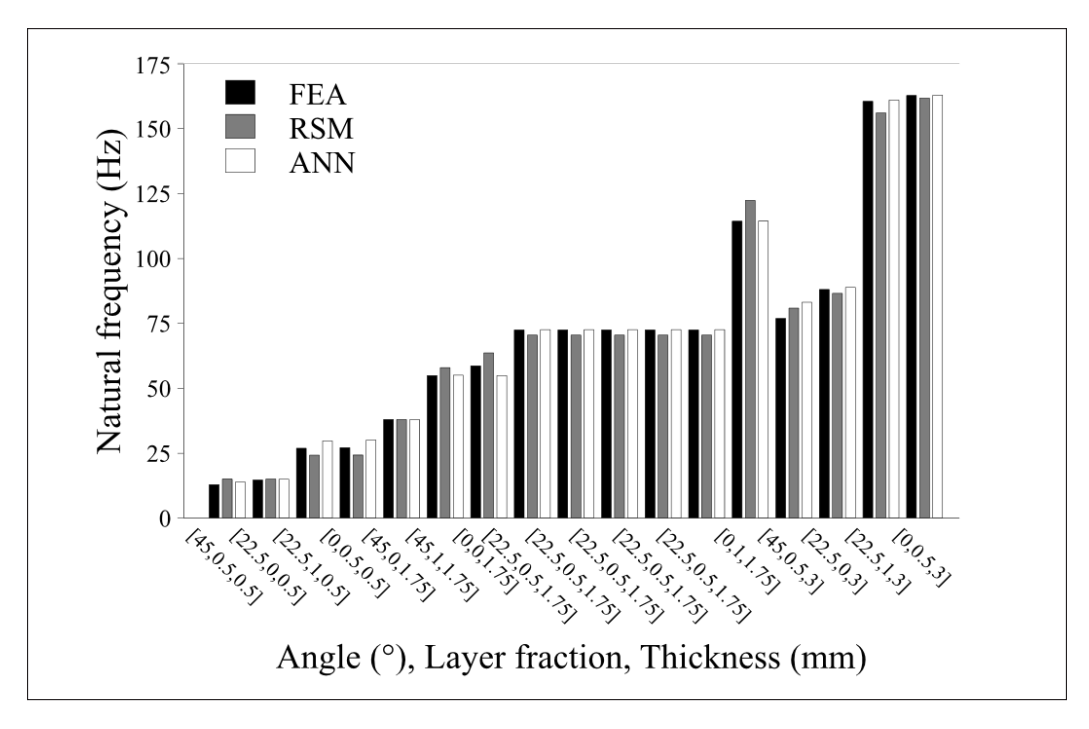


Figure 10. Comparison of natural frequency between the finite element analysis (FEA), response surface method (RSM), and artificial neural network (ANN)

of 0.9986, indicating accurate predictions, while the validation dataset shows a high *R* value of 0.99712, reflecting strong predictive performance. The model demonstrates accuracy and reliability, evidenced by a total *R* value of 0.99682 across the dataset. This study utilises a model summary that integrates Simulink with an ANN to predict natural frequencies. The utilised algorithms comprise the LM training algorithm, random data partitioning, and performance evaluation based on MSE. The accuracy of the ANN model in predicting natural frequencies is demonstrated in Table 4, with percentage errors typically remaining below 10.78%. The increased accuracy demonstrates the model's reliability, as shown in Figure 10. The model demonstrates accuracy, as most samples show errors below 1%. The predicts produced by ANSYS and ANN demonstrate considerable consistency. This agreement, which closely corresponds with the ANSYS results, indicates that the ANN accurately predicts natural frequencies.

Figure 10 compares the predicted natural frequencies obtained through two distinct methods. The predictions are predominantly aligned, with FEA's estimates marginally exceeding those of RSM. The intricate correlation between natural frequency and laminate factors, angle orientation, layer fraction, and plate thickness is emphasised by the initial peak in the bar graph, followed by a decline and subsequent increase in values. This pattern was arranged by increasing plate thickness, followed by layer fraction and angle

orientation. However, the initial spike offers critical insights for structural analysis and design optimisation by identifying factor combinations that significantly influence the stiffness and dynamic behaviour of the laminate. Thus, the initial spike indicates that low-thickness, completely carbon has provided high natural frequencies at 0°. The results of the present study align well with past studies (Njim et al., 2021; Rosaidi et al., 2023; Subrahmanyam et al., 2021).

CONCLUSION

This study illustrates the predictive abilities of ANN and RSM in examining the behaviour of hybrid composite laminates subjected to free vibration conditions. The models created through these methods exhibit differing levels of accuracy in predicting the system's responses, with the ANN model typically surpassing RSM regarding prediction accuracy. The accuracy of prediction is assessed using percentage error, offering a quantitative measure of the deviation between predicted and experimental results.

- i. The ANN model demonstrated a low average percentage error of 2.81%, reflecting its effectiveness in identifying the underlying patterns within the data. Conversely, RSM exhibited a higher average percentage error of 4.96%. However, it still yielded valuable insights into the system's behaviour and functioned as a useful tool for preliminary analysis.
- ii. The study identified that plate thickness significantly influences the free vibration of hybrid composite laminates, with layer fraction following as the next most impactful factor.
- iii. This finding is essential for optimising laminate design for applications, guaranteeing the desired performance characteristics, including stability and resonance frequency.
- iv. ANN demonstrate significant efficacy in managing complex, non-linear relationships and acquiring knowledge from extensive datasets, establishing itself as a formidable instrument in this field.
- v. RSM provides a less complex and more straightforward approach, proving effective in situations where a simpler model suffices. The capacity to adjust to complex interactions among various variables renders it a suitable method for predicting the behaviour of composite materials in vibration analysis.

Both ANN and RSM significantly contribute to the study of hybrid composite laminates, each exhibiting distinct strengths. ANN demonstrate superior accuracy and flexibility, whereas RSM offers a dependable approach for preliminary evaluations and the optimisation of design factors. This study's findings emphasise the necessity of choosing

a suitable modelling technique according to the problem's complexity and the accuracy needed for the intended application. Future studies may concentrate on enhancing model calibration, investigating hybrid methodologies, or incorporating real-time data to achieve more reliable predictions.

ACKNOWLEDGEMENTS

The study has been funded by the Ministry of Higher Education of Malaysia under the Fundamental Research Grant Scheme (Grant no.: FRGS/1/2023/TK10/UITM/02/8).

REFERENCES

- Alam, M. A., Ya, H. H., Azeem, M., Hussain, P. B., Salit, M. S., Khan, R., Arif, S., & Ansari, A. H. (2020). Modelling and optimisation of hardness behaviour of sintered Al/SiC composites using RSM and ANN: A comparative study. *Journal of Materials Research and Technology*, *9*(6), 14036–14050. https://doi.org/10.1016/j.jmrt.2020.09.087
- An, H., Chen, S., & Huang, H. (2019). Multi-objective optimal design of hybrid composite laminates for minimum cost and maximum fundamental frequency and frequency gaps. *Composite Structures*, 209, 268–276. https://doi.org/10.1016/j.compstruct.2018.10.075
- Antony, J. (2014). *Design of experiments for engineers and scientists* (2nd ed.). Elsevier. https://doi.org/10.1016/ C2012-0-03558-2
- Arunachalam, S. J., Saravanan, R., Sathish, T., Giri, J., & Kanan, M. (2024). Mechanical assessment for enhancing hybrid composite performance through silane treatment using RSM and ANN. *Results in Engineering*, 24, 103309. https://doi.org/10.1016/j.rineng.2024.103309
- Arvinda Pandian, C. K., & Jailani, H. S. (2021). Formulation and characterisation of jute fabric–linen fabric–fumed silica–epoxy hybrid laminates. *Journal of the Textile Institute*, 113(1), 151–158. https://doi.org/10.1080/00405000.2020.1866271
- Bezerra, M. A., Santelli, R. E., Oliveira, E. P., Villar, L. S., & Escaleira, L. A. (2008). Response surface methodology (RSM) as a tool for optimization in analytical chemistry. *Talanta*, 76(5), 965–977. https://doi.org/10.1016/j.talanta.2008.05.019
- Boukarma, L., Aboussabek, A., El Aroussi, F., Zerbet, M., Sinan, F., & Chiban, M. (2023). Insight into mechanism, Box-Behnken design, and artificial neural network of cationic dye biosorption by marine macroalgae *Fucus spiralis*. *Algal Research*, 76, 103324. https://doi.org/10.1016/j.algal.2023.103324
- Box, G. E. P., & Behnken, D. W. (1960). Some new three level designs for the study of quantitative variables. *Technometrics*, 2(4), 455–475. https://doi.org/10.1080/00401706.1960.10489912
- Bulut, M., Erkliğ, A., & Yeter, E. (2016). Experimental investigation on influence of Kevlar fiber hybridization on tensile and damping response of Kevlar/glass/epoxy resin composite laminates. *Journal of Composite Materials*, 50(14), 1875–1886. https://doi.org/10.1177/0021998315597552

- Chisena, R. S., Chen, L., & Shih, A. J. (2021). Finite element composite simplification modeling and design of the material extrusion wave infill for thin-walled structures. *International Journal of Mechanical Sciences*, 196, 106–276. https://doi.org/10.1016/j.ijmecsci.2021.106276
- Crawley, E. F. (1979). The natural modes of graphite/epoxy cantilever plates and shells. *Journal of Composite Materials*, 13(3), 195–205. https://doi.org/10.1177/002199837901300302
- de Paula Ferreira, W., Armellini, F., & De Santa-Eulalia, L. A. (2020). Simulation in industry 4.0: A state-of-the-art review. *Computers and Industrial Engineering*, 149, 106868. https://doi.org/10.1016/j.cie.2020.106868
- Erkli, A., Bulut, M., & Yeter, E. (2015). The effect of hybridization and boundary conditions on damping and free vibration of composite plates. *Science and Engineering of Composite Materials*, 22(5), 565–571. https://doi.org/10.1515/secm-2014-0070
- Jadee, K. J., Abed, B. H., & Battawi, A. A. (2020). Free vibration of isotropic plates with various cutout configurations using finite elements and design of experiments. In *IOP Conference Series: Materials Science and Engineering* (Vol. 745, No. 1, p. 012080). IOP Publishing. https://doi.org/10.1088/1757-899X/745/1/012080
- Kallannavar, V., Kumaran, B., & Kattimani, S. C. (2020). Effect of temperature and moisture on free vibration characteristics of skew laminated hybrid composite and sandwich plates. *Thin-Walled Structures*, 157, 107113. https://doi.org/10.1016/j.tws.2020.107113
- Kumar C, H., & Swamy, R. P. (2021). Fatigue life prediction of glass fiber reinforced epoxy composites using artificial neural networks. *Composites Communications*, 26, 100812. https://doi.org/10.1016/j. coco.2021.100812
- Leissa, A. W. (1973). The free vibration of rectangular plates. *Journal of Sound and Vibration*, 31(3), 257–293. https://doi.org/10.1016/S0022-460X(73)80371-2
- Li, M., Soares, C. G., Liu, Z., & Zhang, P. (2024). Free and forced vibration analysis of carbon/glass hybrid composite laminated plates under arbitrary boundary conditions. *Applied Composite Materials*, *31*, 1687–1710. https://doi.org/10.1007/s10443-024-10235-y
- Ma, J., & Gao, H. (2024). Free vibration analysis of hybrid laminated thin-walled cylindrical shells containing multilayer FG-CNTRC plies. Acta Mechanica, 235, 7711–7731. https://doi.org/10.1007/s00707-024-04082-y
- Malik, M. H., & Arif, A. F. M. (2013). ANN prediction model for composite plates against low velocity impact loads using finite element analysis. *Composite Structures*, 101, 290–300. https://doi.org/10.1016/j. compstruct.2013.02.020
- Mallick, A., Mandal, R., Mondal, N., Sarkar, S., Biswas, N., Maji, B., & Majumdar, G. (2024). Parametric optimization and minimization of corrosion rate of electroless Ni–P coating using Box-Behnken design and Artificial Neural Network. *Results in Surfaces and Interfaces*, 15, 100228. https://doi.org/10.1016/j.rsurfi.2024.100228
- Mat Jusoh, S., Zulkifli, M. F. R., Abdullah, S., Shafi, A. R., Mohd Nasir, M. F., Maulana, U. N., Mohd Radzi, F. S., & Zainulabidin, S. H. (2024). Response Surface Methodology for optimisation of factor on water absorption of natural fibre hybrid composite in boat construction. *Pertanika Journal of Science and Technology*, 32(S5), 123–132. https://doi.org/10.47836/pjst.32.S5.06

- Mengistu, A., Andualem, G., Abewaa, M., & Birhane, D. (2024). Keratin extraction optimization from poultry feather using response surface-Box-Behnken experimental design method. *Results in Engineering*, 22, 102360. https://doi.org/10.1016/j.rineng.2024.102360
- Merzuki, M. N. M., Rejab, M. R. M., Sani, M. S. M., Zhang, B., & Quanjin, M. (2019). Experimental investigation of free vibration analysis on fibre metal composite laminates. *Journal of Mechanical Engineering and Sciences*, 13(4), 5753–5763.
- Mirziyod, M., Ibrokhimovich, S. I., & Khudoyberdievich, T. M. (2019). Dynamics of structural-inhomogeneous laminate and shell mechanical systems with point constraints and focused masses. Part 2. Statement of the problem of forced oscillations, methods of solution, computational algorithm and numerical results. *Journal of Applied Mathematics and Physics*, 7(11), 2671–2684. https://doi.org/10.4236/jamp.2019.711182
- Müzel, S. D., Bonhin, E. P., Guimarães, N. M., & Guidi, E. S. (2020). Application of the finite element method in the analysis of composite materials: A review. *Polymers*, 12(4), 818. https://doi.org/10.3390/ POLYM12040818
- Njim, E. K., Bakhy, S. H., & Al-Waily, M. (2021). Analytical and numerical investigation of free vibration behavior for sandwich plate with functionally graded porous metal core. *Pertanika Journal of Science and Technology*, 29(3), 1655–1682. https://doi.org/10.47836/pjst.29.3.39
- Norman, M. A. M., & Mahmud, J. (2021). Investigation of natural frequencies on Kevlar/glass hybrid laminated composite plates using finite element simulation. *International Transaction Journal of Engineering, Management, and Applied Sciences and Technologies*, 12(9), 1–8. https://doi.org/10.14456/ITJEMAST.2021.169
- Norman, M. A. M., Sivakumar, K., Ab Patar, M. N. A., & Mahmud, J. (2022). A prediction model for natural frequencies on Kevlar/glass hybrid laminated composite using Artificial Neural Networks (ANN). *International Journal of Integrated Engineering*, 14(5), 207–214. https://doi.org/10.30880/ ijie.2022.14.05.023
- Norman M. A. M., Zainuddin M. A., & Jamaluddin, M. (2018). The effect of various fiber orientations and boundary conditions on natural frequencies of laminated composite Beam. *International Journal of Engineering and Technology*, 7(3.11), 67–71. https://doi.org/10.14419/jjet.v7i3.11.15932
- Polat, S., & Sayan, P. (2019). Application of response surface methodology with a Box–Behnken design for struvite precipitation. Advanced Powder Technology, 30(10), 2396–2407. https://doi.org/10.1016/j. apt.2019.07.022
- Pratap, B., Mondal, S., & Rao, B. H. (2024). Prediction of compressive strength of bauxite residue-based geopolymer mortar as pavement composite materials: An integrated ANN and RSM approach. *Asian Journal of Civil Engineering*, 25, 597–607. https://doi.org/10.1007/s42107-023-00797-w
- Pushparaj, P., & Suresha, B. (2016). Free vibration analysis of laminated composite plates using finite element method. *Polymers and Polymer Composites*, 24(7), 529–538. https://doi.org/10.1177/096739111602400712
- Quanjin, M., Merzuki, M. N. M., Rejab, M. R. M., Sani, M. S. M., & Zhang, B. (2022). Numerical investigation on free vibration analysis of Kevlar/glass/epoxy resin hybrid composite laminates. *Malaysian Journal on Composites Science and Manufacturing*, *9*(1), 11–21. https://doi.org/10.37934/mjcsm.9.1.1121

- Ratnaparkhi, S. U., & Sarnobat, S. S. (2013). Vibration analysis of composite plate. *International Journal of Modern Engineering Research*, 3(1), 377–380.
- Reddy, B. S., Reddy, M. R. S., & Reddy, V. N. (2013). Vibration analysis of laminated composite plates using design of experiments approach. *International Journal of Scientific Engineering and Technology*, 2(1), 40–49.
- Reddy, M. R. S., Reddy, B. S., Reddy, V. N., & Sreenivasulu, S. (2012). Prediction of natural frequency of laminated composite plates using artificial neural networks. *Engineering*, 4(6), 329–337. https://doi. org/10.4236/eng.2012.46043
- Rosaidi, M. H. M., Mahmud, J., Abdul Rahman, S. M., Abdul Halim, N. H., Raja Abdullah, R. I., & Ab Patar, M. N. A. (2023). Natural frequencies optimisation of hybrid composite laminates using Response Surface Method. *Journal of Advanced Research in Applied Sciences and Engineering Technology*, 31(2), 197–209. https://doi.org/10.37934/araset.31.2.197209
- Safri, S. N. A., Sultan, M. T. H., Jawaid, M., & Jayakrishna, K. (2018). Impact behaviour of hybrid composites for structural applications: A review. *Composites Part B Engineering*, *133*, 112–121. https://doi.org/10.1016/j.compositesb.2017.09.008
- Sai Vivek, K. (2016). Free vibration of skew laminated composite plates with circular cutout by finite element method. *International Journal of Modern Engineering Research*, 6(6), 15–23.
- Samsudin, A. H., & Mahmud, J. (2015). The effect of lamination scheme and angle variations to the displacements and failure behaviour of composite laminate. *Journal Technology Science Engineering*, 76(11), 113–121. https://doi.org/10.11113/jt.v76.5921
- Saravanakumar, S., Sathiyamurthy, S., Pathmanaban, P., & Devi, P. (2024). Integrating machine learning and response surface methodology for analyzing anisotropic mechanical properties of biocomposites. *Composite Interfaces*, 31(1), 1–28. https://doi.org/10.1080/09276440.2023.2260239
- Sathishkumar, N., Selvam, R., Kumar, K. M., Abishini, A. H., Rahman, T. K., & Mohanaranga, S. (2022). Influence of garnet abrasive in drilling of Basalt–Kevlar–Glass fiber reinforced polymer cross ply laminate by Abrasive Water Jet Machining process. *Materials Today: Proceedings*, 62(Part 2), 1361–1368. https://doi.org/10.1016/j.matpr.2022.04.861
- Shi, D., He, D., Wang, Q., Ma, C., & Shu, H. (2020). Free vibration analysis of closed moderately thick crossply composite laminated cylindrical shell with arbitrary boundary conditions. *Materials*, *13*(4), 884. https://doi.org/10.3390/ma13040884
- Shokuhfar, A., Khalili, S. M. R., Ashenai Ghasemi, F., Malekzadeh, K., & Raissi, S. (2008). Analysis and optimization of smart hybrid composite plates subjected to low-velocity impact using the response surface methodology (RSM). *Thin-Walled Structures*, 46(11), 1204–1212. https://doi.org/10.1016/j. tws.2008.02.007
- Sreekanth, T. G., Senthilkumar, M., & Reddy, S. M. (2023). Artificial neural network based delamination prediction in composite plates using vibration signals. *Fracture and Structural Integrity*, 17(63), 37–45. https://doi.org/10.3221/IGF-ESIS.63.04

- Subrahmanyam, A. P. S. V. R., Srinivasa Rao, P., & Siva Prasad, K. (2021). Enhancement of surface quality of DMLS aluminium alloy using RSM optimization and ANN modelling. *Journal of Mechanical Engineering*, 18(3), 37–56.
- Swamy, G. J., Sangamithra, A., & Chandrasekar, V. (2014). Response surface modeling and process optimization of aqueous extraction of natural pigments from *Beta vulgaris* using Box-Behnken design of experiments. *Dyes and Pigments*, 111, 64–74. https://doi.org/10.1016/j.dyepig.2014.05.028
- Triefenbach, F. (2008). *Design of experiments: The D-optimal approach and its implementation as a computer algorithm* [Unpublished Bachelor's dissertation]. South Westphalia University of Applied Sciences.
- Warburton, G. B. (1954). The vibration of rectangular plates. *Proceedings of the Institution of Mechanical Engineers*, 168(1), 371–384. https://doi.org/10.1243/pime_proc_1954_168_040_02